Int. J. Adv. Appl. Math. and Mech. 2(3) (2015) 183 - 195 (ISSN: 2347-2529)
Journal homepage: www.ijaamm.com

International Journal of Advances in Applied Mathematics and Mechanics

Mathematical modelling of thermoelastic problem in a circular sector disk subject to heat generation

Research Article

Kishor R. Gaikwad *

Post Graduate Department of Mathematics, NES, Science College, Nanded-431602, Maharashtra, India.

Received 02 February 2015; accepted (in revised version) 27 February 2015

Abstract: The present paper deals with the determination of temperature, displacement and thermal stresses in a circular sector disk defined as $0 \le r \le a$, $0 \le \varphi \le \varphi_0 < 2\pi$, $0 \le z \le h$ under an unsteady-state temperature field, due to internal heat generation within it. The time dependent heat flux $f_1(\varphi, z, t)$ is applied on the fixed circular edge $(r = a)$. For time $t > 0$, the boundary surfaces at $(\varphi = 0)$, $(\varphi = \varphi_0)$, $(z = 0)$ and $(z = h)$ are maintained at a prescribed temperatures $f_2(r, z, t)$, $f_3(r, z, t)$, $f_4(r, \varphi, t)$ and $f_5(r, \varphi, t)$ respectively, while the entire volume is subjected to internal energy generation given by the function $g(r, \varphi, z, t)$. The governing heat conduction equation has been solved by using finite Hankel transform and the generalized finite Fourier transform technique. As a special case mathematical model is constructed for pure aluminium circular sector disk considered. The results are obtained in series form in terms of Bessel's functions. These have been computed numerically and illustrated graphically.

MSC: 35B07 • 35G30 • 35K05 • 44A10

Keywords: Thermoelastic Problem • Circular Sector Disk • Heat Generation • Unsteady-State Temperature

1. Introduction

During the second half of the twentieth century, non-isothermal problems of the theory of elasticity became increasingly important. This is mainly due to their many applications in widely diverse fields. First, the high velocities of modern aircraft give rise to aerodynamic heating, which produces intense thermal stresses, reducing the strength of the aircraft structure. Second, in the nuclear field, the extremely high temperatures and temperature gradients originating inside nuclear reactors influence their design and operations [1].

Nowacki [2] has determined the steady-state thermal stresses in a circular plate subjected to an axisymmetric temperature distribution on the upper surface with zero temperature on the lower surface and with the circular edge thermally insulated. Roy Choudhury [3] discussed the quasi-static thermal deflection of a thin clamped circular plate due to ramp type heating of a concentric circular region of the upper face, with the lower surface is kept at zero temperature and circular edge thermally insulated. Wankhede [4] determined the arbitrary temperature on the upper face with the lower face at zero temperature and the fixed circular edge thermally insulated. Ishihara at al. [5] discussed the theoretical analysis of thermoelastoplastic deformation of a circular plate due to a partially distributed heat supply. Khobragade et al. [6] solved an inverse axially symmetric quasi-static problem of thermoelasticity for a thin clamped circular plate in which a heat flux is prescribed on an internal cylindrical surface of the plate and suitable heat exchange conditions are met on the upper and lower surfaces of the plate is solved with the help of a generalized integral transform technique. Ootao and Tanigawa [7] have studied the transient thermoelastic analysis for a functionally graded hollow cylinder due to uniform heat supply. Deshmukh

* Corresponding author.
E-mail address: drkr.gaikwad@yahoo.in

et al. [8] have studied the two dimensional non-homogeneous boundary value problem of heat conduction and studied the thermal deflection of a thin clamped circular plate due to heat generation.

Gaikwad et al. [9] solved the quasi-static thermal stresses of an infinitely long circular cylinder having constant initial temperature under steady-state temperature field. Parihar and Patil [10] presented results for the thermoelastic problems of thin circular and rectangular plates. Gaikwad et al. [11] have solved nonhomogeneous heat conduction problem and obtained thermal deflection due to internal heat generation in a thin hollow circular disk. Gaikwad [12] analysed thermoelastic deformation of a thin hollow circular disk due to partially distributed heat supply. Darji and Timol [13] have studied thedeductive group symmetry analysis for a free convective boundary-layer flow of electrically conducting non-Newtonian fluids over a vertical porous-elastic surface. Also, Gnaneswara Reddy [14] investigated the heat and mass transfer effects on unsteady MHD flow of a chemically reacting fluid past an impulsively started vertical plate with radiation. Recently, M. F. El-sayed et al. [15] studied the nonlinear stability of viscoelastic fluids streaming through porous medium under the influence of vertical electric fields producing surface charges.

The present article is concerned with a quasi-static thermal stresses in a circular sector disk occupying the space D: $0 \le r \le a, 0 \le \varphi \le \varphi_0 < 2\pi, 0 \le z \le h$, under unsteady-state temperature field due to internal heat generation within it. The time dependent heat flux $f_1(\varphi, z, t)$ is applied on the fixed circular edge $(r = a)$. For time $t > 0$, the boundary surfaces at $(\varphi = 0)$, $(\varphi = \varphi_0)$, $(z = 0)$ and $(z = h)$ are maintained at a prescribed temperatures $f_2(r, z, t)$, $f_3(r, z, t)$, $f_4(r, \varphi, t)$ and $f_5(r, \varphi, t)$ respectively, while the entire volume is subjected to internal energy generation given by the function $g(r, \varphi, z, t)$. The governing heat conduction equation has been solved by using finite Hankel transform and the generalized finite Fourier transform technique. In the given problem we examined two cases. In first case, initially the disk is at arbitrary temperature $F(r, \varphi, z)$ and in second case, initially the disk is at zero temperature. As a special case mathematical model is constructed for pure aluminium circular sector disk considered. The results are obtained in series form in terms of Bessel functions. These have been computed numerically and illustrated graphically.

To the author's knowledge, no one has considered the problem of the circular sector disk and studied the displacement and thermal stresses due to internal heat generation in a circular sector disk. This is a new and novel contribution to the field of thermoelasticity. The results presented here displacement and thermal stresses that are obtained can be applied to the design of useful structure or machines in engineering application.

2. Mathematical formulation of the problem

Consider a circular sector disk occupying the space D: $0 \le r \le a$, $0 \le \varphi \le \varphi_0 < 2\pi$, $0 \le z \le h$, see Fig. 1. The time dependent heat flux $f_1(\varphi, z, t)$ is applied on the fixed circular edge $(r = a)$. For time $t > 0$, the boundary surfaces at $(\varphi = 0)$, $(\varphi = \varphi_0)$, $(z = 0)$ and $(z = h)$ are maintained at a prescribed temperatures $f_2(r, z, t)$, $f_3(r, z, t)$, $f_4(r, \varphi, t)$ and $f_5(r, \varphi, t)$ respectively, while the entire volume is subjected to internal energy generation given by the function $g(r, \varphi, z, t)$. Under these prescribed conditions, temperature, displacement and thermal stresses in a circular sector disk due to internal heat generation are required to be determined.
The boundary value problem of the heat conduction is given as

$$\frac{\partial^2 T}{\partial r^2} + \frac{1}{r}\frac{\partial T}{\partial r} + \frac{1}{r^2}\frac{\partial^2 T}{\partial \varphi^2} + \frac{\partial^2 T}{\partial z^2} + \frac{g(r, \varphi, t)}{k} = \frac{1}{\alpha}\frac{\partial T}{\partial t} \qquad \text{in } 0 \le r \le a, 0 \le \varphi \le \varphi_0 < 2\pi, 0 \le z \le h, t > 0 \tag{1}$$

subject to the boundary conditions

$$k\frac{\partial T}{\partial r} = f_1(\varphi, z, t) \qquad \text{at } r = a, t > 0 \tag{2}$$

$$T = f_2(r, z, t) \qquad \text{at } \varphi = 0, t > 0 \tag{3}$$

$$T = f_3(r, z, t) \qquad \text{at } \varphi = \varphi_0, t > 0 \tag{4}$$

$$T = f_4(r, \varphi, t) \qquad \text{at } z = 0, t > 0 \tag{5}$$

$$T = f_5(r, \varphi, t) \qquad \text{ar } z = h, t > 0 \tag{6}$$

and initial condition

$$T = F(r, \varphi, z) \qquad \text{at } t = 0 \tag{7}$$

where $T = T(r, \varphi, z, t)$ and k, α are the thermal conductivity and thermal diffusivity of the material of the circular sector disk. Following Roy Choudhary [3], we assume that for small thickness h the circular disk is in a plane state of stress. In fact "the smaller the thickness of the disk compared to its diameter, the nearer to a plane state of stress is the actual state". The displacement equations of thermoelasticity have the form,

$$U_{i,kk} + \left(\frac{1+\nu}{1-\nu}\right)e_{,i} = 2\left(\frac{1+\nu}{1-\nu}\right)a_t T_{,i}$$

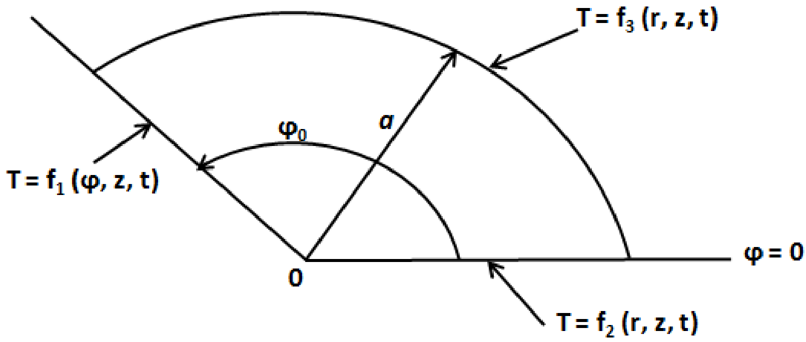

Fig. 1. The geometry of the problem.

$$e = U_{k,k} \quad k, i = 1, 2,$$

where U_i is the displacements component, e is the dilatation, T is the temperature and ν and a_t are respectively, the Poisson's ratio and linear coefficient of thermal expansion of the disk material.
Introducing

$$U_i = \psi_{,i}, \quad i = 1, 2,$$

we have

$$\nabla_1^2 \psi = (1+\nu) a_t T$$

$$\nabla_1^2 = \frac{\partial^2}{\partial x_1^2} + \frac{\partial^2}{\partial x_2^2}$$

The stress σ_{ij} is given by

$$\sigma_{ij} = 2\mu(\psi_{,ij} - \delta_{ij}\psi_{,kk}), \qquad i, j, k = 1, 2,$$

where μ is Lamé constant and δ_{ij} is the Kronecker delta symbol.
The differential equation governing the displacement potential function $\psi(r, \varphi, z, t)$ is expressed as

$$\frac{\partial^2 \psi}{\partial r^2} + \frac{1}{r}\frac{\partial \psi}{\partial r} = (1+\nu) a_t T \tag{8}$$

$$\text{with} \quad \frac{\partial \psi}{\partial r} = 0 \qquad \text{at } r = a \quad \text{for all time } t. \tag{9}$$

$$\text{Initially} \quad T = \psi = F(r, \varphi, z) \qquad \text{at } t = 0. \tag{10}$$

The stress functions σ_{rr} and $\sigma_{\theta\theta}$ are given by,

$$\sigma_{rr} = -\frac{2\mu}{r}\frac{\partial \psi}{\partial r} \tag{11}$$

$$\sigma_{\theta\theta} = -2\mu \frac{\partial^2 \psi}{\partial r^2} \tag{12}$$

The traction-free boundary conditions for the circular sector disk in the form

$$\sigma_{rr} = \sigma_{r\varphi} = 0 \qquad \text{for } r = a, 0 \le \varphi < \varphi_0, \ t > 0 \tag{13}$$

$$\sigma_{\varphi\varphi} = \sigma_{r\varphi} = 0 \qquad \text{for } 0 \le r < a, \ \varphi = 0, \ t > 0 \tag{14}$$

$$\sigma_{\varphi\varphi} = \sigma_{r\varphi} = 0 \qquad \text{for } 0 \le r < a, \ \varphi = \varphi_0, \ t > 0 \tag{15}$$

Equations (1) to (15) constitute the mathematical formulation of the problem under consideration.

3. Solution of the heat conduction problem

To obtain the expression for temperature function $T(r,\varphi,z,t)$; firstly we define the finite Fourier transform and its inverse transform over the variable z in the range $0 \le z \le h$ defined in [16] as,

$$\overline{T}(r,\varphi,\eta_p,t)=\int_{z'=0}^{h} K(\eta_p,z')\,T(r,\varphi,z',t)\,dz' \tag{16}$$

$$T(r,\varphi,z,t)=\sum_{n=1}^{\infty} K(\eta_p,z)\,\overline{T}(r,\varphi,\eta_p,t) \tag{17}$$

where

$$K(\eta_p,z)=\sqrt{\frac{2}{h}}\,\sin(\eta_p z)$$

and $\eta_1,\eta_2,\ldots$ are the positive roots of the transcendental equation

$$\sin(\eta_p h)=0,\quad p=1,2,3,\ldots$$

i.e.

$$\eta_p=\frac{p\pi}{h},\quad p=1,2,3,\ldots$$

Applying the finite Fourier transform defined in equation (16) to equation (1) and using the conditions (2)?-(7), one obtains

$$\frac{\partial^2\overline{T}}{\partial r^2}+\frac{1}{r}\frac{\partial\overline{T}}{\partial r}+\frac{1}{r^2}\frac{\partial^2\overline{T}}{\partial\varphi^2}-\eta_p^2\,\overline{T}+\frac{\overline{g}(r,\varphi,\eta_p,t)}{K}=\frac{1}{\alpha}\frac{\partial\overline{T}}{\partial t} \tag{18}$$

the boundary conditions

$$k\frac{\partial\overline{T}}{\partial r}=\overline{f}_1(\varphi,\eta_p,t)\qquad \text{at } r=a,\ t>0 \tag{19}$$

$$\overline{T}=\overline{f}_2(r,\eta_p,t)\qquad \text{at } \varphi=0,\ t>0 \tag{20}$$

$$\overline{T}=\overline{f}_3(r,\eta_p,t)\qquad \text{at } \varphi=\varphi_0,\ t>0 \tag{21}$$

with

$$\overline{T}=\overline{F}(r,\varphi,\eta_p)\qquad \text{at } t=0 \tag{22}$$

Secondly, we define the finite Fourier transform and its inverse transform over the variable φ in the range $0\le\varphi\le\varphi_0$ defined in [16] as,

$$\overline{\overline{T}}(r,\nu,\eta_p,t)=\int_{\varphi'=0}^{\varphi_0} K_0(\nu,\varphi')\,\overline{T}(r,\varphi',\eta_p,t)\,d\varphi' \tag{23}$$

$$\overline{T}(r,\varphi,\eta_p,t)=\sum_{\nu} K_0(\nu,\varphi)\overline{\overline{T}}(r,\nu,\eta_p,t) \tag{24}$$

where

$$K_0(\nu,\varphi)=\sqrt{\frac{2}{\varphi_0}}\,\sin(\nu\varphi)$$

and the eigenvalues ν are the positive roots of

$$\sin(\nu\varphi_0)=0$$

i.e.

$$\nu = \frac{n\pi}{\varphi_0}, \quad n = 1,2,3\ldots$$

Applying the finite Fourier transform defined in equation (23) to equation (18) and using the conditions (19)?-(22), one obtains

$$\frac{\partial^2 \overline{\overline{T}}}{\partial r^2} + \frac{1}{r}\frac{\partial \overline{\overline{T}}}{\partial r} - \frac{\nu^2}{r^2}\overline{\overline{T}} - \eta_p^2\,\overline{\overline{T}} + \frac{\overline{\overline{g}}(r,\nu,\eta_p,t)}{K} = \frac{1}{\alpha}\frac{\partial \overline{\overline{T}}}{\partial t} \tag{25}$$

with

$$k\frac{\partial \overline{\overline{T}}}{\partial r} = \overline{\overline{f}}_1(\nu,\eta_p,t) \qquad \text{at } r = a,\ t > 0 \tag{26}$$

$$\overline{\overline{T}} = \overline{\overline{F}}(r,\nu,\eta_p) \qquad \text{at } t = 0 \tag{27}$$

Lastly, we define finite Hankel transform and its inverse transform over the variable r in the range $0 \le r < a$ as defined in [16] respectively as,

$$\overline{\overline{\overline{T}}}(\beta_m,\nu,\eta_p,t) = \int_{r'=0}^{a} r' K_1(\beta_m,r')\,\overline{\overline{T}}(r',\nu,\eta_p,t)\,dr' \tag{28}$$

$$\overline{\overline{T}}(r,\nu,\eta_p,t) = \sum_{m=1}^{\infty} K_1(\beta_m,r)\,\overline{\overline{\overline{T}}}(\beta_m,\nu,\eta_p,t) \tag{29}$$

where

$$K_1(\beta_m,r) = \frac{\sqrt{2}}{a}\,\frac{J_0(\beta_m r)}{J_0(\beta_m a)}$$

and $\beta_1, \beta_2, \beta_3, \ldots$ are the positive root of transcendental equation

$$J_1(\beta_m a) = 0, \quad m = 1,2,3\ldots$$

Applying the finite Hankel transform defined in equation (28) to equation (25) and using the conditions (26)?-(27), one obtains

$$\frac{\partial \overline{\overline{\overline{T}}}(\beta_m,\nu,\eta_p,t)}{\partial t} + \alpha\left(\beta_m^2 + \frac{\nu^2}{r^2} + \eta_p^2\right)\overline{\overline{\overline{T}}}(\beta_m,\nu,\eta_p,t) = A(\beta_m,\nu,\eta_p,t) \tag{30}$$

with

$$\overline{\overline{\overline{T}}}(\beta_m,\eta_p,t) = \overline{\overline{\overline{F}}}(\beta_m,\nu,\eta_p) \qquad \text{for } t = 0, \tag{31}$$

where

$$\begin{aligned} A(\beta_m,\nu,\eta_p,t) = {}& \frac{\alpha}{k}\,\overline{\overline{\overline{g}}}(\beta_m,\nu,\eta_p,t) + \frac{\alpha}{k}\,a\,K_1(\beta_m,a)\,\overline{\overline{f}}_1(\nu,\eta_p,t) \\ & \left\{\frac{dK_0(\nu,\varphi)}{d\varphi}\,\overline{\overline{f}}_2(\beta_m,\eta_p,t)\Big|_{\varphi=0} - \frac{dK_0(\nu,\varphi)}{d\varphi}\,\overline{\overline{f}}_3(\beta_m,\eta_p,t)\Big|_{\varphi=\varphi_0}\right. \\ & \left. + \frac{dK(\eta_p,z)}{dz}\,\overline{\overline{f}}_4(\beta_m,\nu,t)\Big|_{z=0} + \frac{dK(\eta_p,z)}{dz}\,\overline{\overline{f}}_5(\beta_m,\nu,t)\Big|_{z=h}\right\} \end{aligned} \tag{32}$$

Solution of the equation (32) is obtained as

$$\overline{\overline{\overline{T}}}(\beta_m,\nu,\eta_p,t) = e^{-\alpha(\beta_m^2+\frac{\nu^2}{r^2}+\eta_p^2)t}\left[\overline{\overline{\overline{F}}}(\beta_m,\nu,\eta_p) + \int_{t'=0}^{t} e^{\alpha(\beta_m^2+\frac{\nu^2}{r^2}+\eta_p^2)t'} A(\beta_m,\nu,\eta_p,t')\,dt'\right] \tag{33}$$

Finally, taking the inverse finite Hankel transform defined in equation (29) and inverse finite Fourier transform defined in equations (24) and (17), one obtains the expressions of the temperature $T(r,\varphi,z,t)$ as

$$
\begin{aligned}
T(r,\varphi,z,t) &= \sum_{m=1}^{\infty}\sum_{\nu}\sum_{p=1}^{\infty} K_1(\beta_m,r)\,K_0(\nu,\varphi)\,K(\eta_p,z)\,e^{-\alpha(\beta_m^2+\frac{\nu^2}{r^2}+\eta_p^2)t} \\
&\left\{\int_{r'=0}^{a}\int_{\varphi'=0}^{\varphi_0}\int_{z'=0}^{h} r'K_1(\beta_m,r')K_0(\nu,\varphi')K(\eta_p,z')F(r',\varphi',z')dr'd\varphi'dz'\right. \\
&+\int_{t'=0}^{t} e^{\alpha(\beta_m^2+\frac{\nu^2}{r^2}+\eta_p^2)t}\left[\frac{\alpha}{k}\int_{r'=0}^{a}\int_{\varphi'=0}^{\varphi_0}\int_{z'=0}^{h} r'K_1(\beta_m,r')K_0(\nu,\varphi')K(\eta_p,z')g(r',\varphi',z',t')dr'd\varphi'dz'\right. \\
&\quad+\frac{\alpha}{k}\,a\,K_1(\beta_m,a)\int_{\varphi'=0}^{\varphi_0}\int_{z'=0}^{h} K_0(\nu,\varphi')K(\eta_p,z')f_1(\varphi',z',t)d\varphi'dz' \\
&\quad+\alpha\,\nu\sqrt{\frac{2}{\varphi_0}}\int_{r'=0}^{a}\int_{z'=0}^{h} r'K_1(\beta_m,r')K(\eta_p,z')f_2(r',z',t')dr'dz' \\
&\quad-\alpha\,\nu\sqrt{\frac{2}{\varphi_0}}\cos(\nu\varphi_0)\int_{r'=0}^{a}\int_{z'=0}^{h} r'K_1(\beta_m,r')K(\eta_p,z')f_3(r',z',t')dr'dz' \\
&\quad+\sqrt{\frac{2}{\pi}}\,\alpha\,\eta_p\int_{r'=0}^{a}\int_{\varphi'=0}^{\varphi_0} r'K_1(\beta_m,r')K_0(\nu,\varphi')f_4(r',\varphi',t')dr'd\varphi' \\
&\quad\left.\left.+\sqrt{\frac{2}{\pi}}\,\alpha\,\eta_p\cos(\eta_p h)\int_{r'=0}^{a}\int_{\varphi'=0}^{\varphi_0} r'K_1(\beta_m,r')K_0(\nu,\varphi')f_5(r',\varphi',t')dr'd\varphi'\right]dt'\right\}
\end{aligned}
\tag{34}
$$

4. Displacement potential function and thermal stresses

To obtain the displacement function ψ, using Eq. (34) in Eq. (8), one obtains

$$
\begin{aligned}
\frac{\partial^2\psi}{\partial r^2}+\frac{1}{r}\frac{\partial\psi}{\partial r} &= (1+\nu)a_t\sum_{m=1}^{\infty}\sum_{\nu}\sum_{p=1}^{\infty} K_1(\beta_m,r)\,K_0(\nu,\varphi)\,K(\eta_p,z)\,e^{-\alpha(\beta_m^2+\frac{\nu^2}{r^2}+\eta_p^2)t} \\
&\left\{\int_{r'=0}^{a}\int_{\varphi'=0}^{\varphi_0}\int_{z'=0}^{h} r'K_1(\beta_m,r')K_0(\nu,\varphi')K(\eta_p,z')F(r',\varphi',z')dr'd\varphi'dz'\right. \\
&+\int_{t'=0}^{t} e^{\alpha(\beta_m^2+\frac{\nu^2}{r^2}+\eta_p^2)t}\left[\frac{\alpha}{k}\int_{r'=0}^{a}\int_{\varphi'=0}^{\varphi_0}\int_{z'=0}^{h} r'K_1(\beta_m,r')K_0(\nu,\varphi')K(\eta_p,z')g(r',\varphi',z',t')dr'd\varphi'dz'\right. \\
&\quad+\frac{\alpha}{k}\,a\,K_1(\beta_m,a)\int_{\varphi'=0}^{\varphi_0}\int_{z'=0}^{h} K_0(\nu,\varphi')K(\eta_p,z')f_1(\varphi',z',t)d\varphi'dz' \\
&\quad+\alpha\,\nu\sqrt{\frac{2}{\varphi_0}}\int_{r'=0}^{a}\int_{z'=0}^{h} r'K_1(\beta_m,r')K(\eta_p,z')f_2(r',z',t')dr'dz' \\
&\quad-\alpha\,\nu\sqrt{\frac{2}{\varphi_0}}\cos(\nu\varphi_0)\int_{r'=0}^{a}\int_{z'=0}^{h} r'K_1(\beta_m,r')K(\eta_p,z')f_3(r',z',t')dr'dz' \\
&\quad+\sqrt{\frac{2}{\pi}}\,\alpha\,\eta_p\int_{r'=0}^{a}\int_{\varphi'=0}^{\varphi_0} r'K_1(\beta_m,r')K_0(\nu,\varphi')f_4(r',\varphi',t')dr'd\varphi' \\
&\quad\left.\left.+\sqrt{\frac{2}{\pi}}\,\alpha\,\eta_p\cos(\eta_p h)\int_{r'=0}^{a}\int_{\varphi'=0}^{\varphi_0} r'K_1(\beta_m,r')K_0(\nu,\varphi')f_5(r',\varphi',t')dr'd\varphi'\right]dt'\right\}
\end{aligned}
\tag{35}
$$

Solving Eq. (35), one obtains

$$
\begin{aligned}
\psi = & -(1+\nu)a_t \sum_{m=1}^{\infty}\sum_{\nu}\sum_{p=1}^{\infty} \frac{1}{\beta_m^2} K_1(\beta_m, r)\, K_0(\nu,\varphi)\, K(\eta_p, z)\, e^{-\alpha(\beta_m^2+\frac{\nu^2}{r^2}+\eta_p^2)t} \\
& \Bigg\{ \int_{r'=0}^{a}\int_{\varphi'=0}^{\varphi_0}\int_{z'=0}^{h} r' K_1(\beta_m, r')K_0(\nu,\varphi')K(\eta_p, z')F(r',\varphi',z')dr'd\varphi'dz' \\
& + \int_{t'=0}^{t} e^{\alpha(\beta_m^2+\frac{\nu^2}{r^2}+\eta_p^2)t} \Bigg[\frac{\alpha}{k}\int_{r'=0}^{a}\int_{\varphi'=0}^{\varphi_0}\int_{z'=0}^{h} r' K_1(\beta_m, r')K_0(\nu,\varphi')K(\eta_p, z')g(r',\varphi',z',t')dr'd\varphi'dz' \\
& \quad + \frac{\alpha}{k}\, a\, K_1(\beta_m, a)\int_{\varphi'=0}^{\varphi_0}\int_{z'=0}^{h} K_0(\nu,\varphi')K(\eta_p, z')f_1(\varphi',z',t)d\varphi'dz' \\
& \quad + \alpha\, \nu\sqrt{\frac{2}{\varphi_0}}\int_{r'=0}^{a}\int_{z'=0}^{h} r' K_1(\beta_m, r')K(\eta_p, z')f_2(r',z',t')dr'dz' \\
& \quad - \alpha\, \nu\sqrt{\frac{2}{\varphi_0}}\cos(\nu\varphi_0)\int_{r'=0}^{a}\int_{z'=0}^{h} r' K_1(\beta_m, r')K(\eta_p, z')f_3(r',z',t')dr'dz' \\
& \quad + \sqrt{\frac{2}{\pi}}\,\alpha\,\eta_p\int_{r'=0}^{a}\int_{\varphi'=0}^{\varphi_0} r' K_1(\beta_m, r')K_0(\nu,\varphi')f_4(r',\varphi',t')dr'd\varphi' \\
& \quad + \sqrt{\frac{2}{\pi}}\,\alpha\,\eta_p\cos(\eta_p h)\int_{r'=0}^{a}\int_{\varphi'=0}^{\varphi_0} r' K_1(\beta_m, r')K_0(\nu,\varphi')f_5(r',\varphi',t')dr'd\varphi' \Bigg] dt' \Bigg\}
\end{aligned}
\tag{36}
$$

Using Eq. (36) in Eqs. (11) and (12), one obtains the expressions of thermal stresses as

$$
\begin{aligned}
\sigma_{rr} = & -2(1+\nu)a_t\,\mu \sum_{m=1}^{\infty}\sum_{\nu}\sum_{p=1}^{\infty} \frac{1}{r\beta_m} K_2(\beta_m, r)\, K_0(\nu,\varphi)\, K(\eta_p, z)\, e^{-\alpha(\beta_m^2+\frac{\nu^2}{r^2}+\eta_p^2)t} \\
& \Bigg\{ \int_{r'=0}^{a}\int_{\varphi'=0}^{\varphi_0}\int_{z'=0}^{h} r' K_1(\beta_m, r')K_0(\nu,\varphi')K(\eta_p, z')F(r',\varphi',z')dr'd\varphi'dz' \\
& + \int_{t'=0}^{t} e^{\alpha(\beta_m^2+\frac{\nu^2}{r^2}+\eta_p^2)t} \Bigg[\frac{\alpha}{k}\int_{r'=0}^{a}\int_{\varphi'=0}^{\varphi_0}\int_{z'=0}^{h} r' K_1(\beta_m, r')K_0(\nu,\varphi')K(\eta_p, z')g(r',\varphi',z',t')dr'd\varphi'dz' \\
& \quad + \frac{\alpha}{k}\, a\, K_1(\beta_m, a)\int_{\varphi'=0}^{\varphi_0}\int_{z'=0}^{h} K_0(\nu,\varphi')K(\eta_p, z')f_1(\varphi',z',t)d\varphi'dz' \\
& \quad + \alpha\, \nu\sqrt{\frac{2}{\varphi_0}}\int_{r'=0}^{a}\int_{z'=0}^{h} r' K_1(\beta_m, r')K(\eta_p, z')f_2(r',z',t')dr'dz' \\
& \quad - \alpha\, \nu\sqrt{\frac{2}{\varphi_0}}\cos(\nu\varphi_0)\int_{r'=0}^{a}\int_{z'=0}^{h} r' K_1(\beta_m, r')K(\eta_p, z')f_3(r',z',t')dr'dz' \\
& \quad + \sqrt{\frac{2}{\pi}}\,\alpha\,\eta_p\int_{r'=0}^{a}\int_{\varphi'=0}^{\varphi_0} r' K_1(\beta_m, r')K_0(\nu,\varphi')f_4(r',\varphi',t')dr'd\varphi' \\
& \quad + \sqrt{\frac{2}{\pi}}\,\alpha\,\eta_p\cos(\eta_p h)\int_{r'=0}^{a}\int_{\varphi'=0}^{\varphi_0} r' K_1(\beta_m, r')K_0(\nu,\varphi')f_5(r',\varphi',t')dr'd\varphi' \Bigg] dt' \Bigg\}
\end{aligned}
\tag{37}
$$

$$\sigma_{\theta\theta}=-2(1+\nu)a_t\mu\sum_{m=1}^{\infty}\sum_{\nu}\sum_{p=1}^{\infty}\frac{1}{\beta_m}\left(\beta_m K_1(\beta_m,r)-\frac{K_2(\beta_m,r)}{r}\right)K_0(\nu,\varphi)K(\eta_p,z)e^{-\alpha(\beta_m^2+\frac{\nu^2}{r^2}+\eta_p^2)t}$$
$$\left\{\int_{r'=0}^{a}\int_{\varphi'=0}^{\varphi_0}\int_{z'=0}^{h} r'K_1(\beta_m,r')K_0(\nu,\varphi')K(\eta_p,z')F(r',\varphi',z')dr'd\varphi'dz'\right.$$
$$+\int_{t'=0}^{t} e^{\alpha(\beta_m^2+\frac{\nu^2}{r^2}+\eta_p^2)t}\left[\frac{\alpha}{k}\int_{r'=0}^{a}\int_{\varphi'=0}^{\varphi_0}\int_{z'=0}^{h} r'K_1(\beta_m,r')K_0(\nu,\varphi')K(\eta_p,z')g(r',\varphi',z',t')dr'd\varphi'dz'\right.$$
$$+\frac{\alpha}{k}\,a\,K_1(\beta_m,a)\int_{\varphi'=0}^{\varphi_0}\int_{z'=0}^{h} K_0(\nu,\varphi')K(\eta_p,z')f_1(\varphi',z',t)d\varphi'dz'$$
$$+\alpha\,\nu\sqrt{\frac{2}{\varphi_0}}\int_{r'=0}^{a}\int_{z'=0}^{h} r'K_1(\beta_m,r')K(\eta_p,z')f_2(r',z',t')dr'dz' \tag{38}$$
$$-\alpha\,\nu\sqrt{\frac{2}{\varphi_0}}\cos(\nu\varphi_0)\int_{r'=0}^{a}\int_{z'=0}^{h} r'K_1(\beta_m,r')K(\eta_p,z')f_3(r',z',t')dr'dz'$$
$$+\sqrt{\frac{2}{\pi}}\,\alpha\,\eta_p\int_{r'=0}^{a}\int_{\varphi'=0}^{\varphi_0} r'K_1(\beta_m,r')K_0(\nu,\varphi')f_4(r',\varphi',t')dr'd\varphi'$$
$$\left.\left.+\sqrt{\frac{2}{\pi}}\,\alpha\,\eta_p\cos(\eta_p h)\int_{r'=0}^{a}\int_{\varphi'=0}^{\varphi_0} r'K_1(\beta_m,r')K_0(\nu,\varphi')f_5(r',\varphi',t')dr'd\varphi'\right]dt'\right\}$$

where

$$K_2(\beta_m,r)=\frac{\partial}{\partial r}[K_1(\beta_m,r)]$$

5. Special cases and numerical calculations

Setting
$f_{1,}(\varphi,z,t)=(\varphi^2-\varphi_0^2)^2(z^2-h^2)^2e^{-At}$
$f_2(r,z,t)=(r^2-a^2)^2(z^2-h^2)^2e^{-At}$
$f_3(r,z,t)=(r^2-a^2)^2(z^2-h^2)^2e^{-At}$
$f_4(r,\varphi,t)=(r^2-a^2)^2(\varphi^2-\varphi_0^2)^2e^{-At}$
$f_5(r,\varphi,t)=(r^2-a^2)^2(\varphi^2-\varphi_0^2)^2e^{-At}$
where r is the radius measured in meter and $A=5\,s^{-1}>0$.

Dimension
The constants associated with the numerical calculation are taken as
Radius of a circular sector disk a = 2 m
Thickness of a circular sector disk h= 0.4 m,
Portion of a circular sector disk φ_0 =270^0
Central circular path of disk in radial and axial directions: r_1 = 1 m, z_1= 0.2 m and φ_1 = 135^0.

Material properties
The numerical calculation has been carried out for an aluminum (Pure) circular sector disk with the material properties as,
Thermal diffusivity $\alpha=84.18$ m^2/s
Thermal conductivity k= 204 W/mK
Density ρ= 2707 kg/m^3
Specific heat capacity c_p=896 J/kg.K
Poisson ratio $\nu=0.35$
Lam$\acute{e}$ constant μ=26.67 GPa
Coefficients of linear thermal expansion a_t = 22.2 $\times 10^{-6}\frac{1}{K}$
Young's modulus elasticity of the material of the disk E = 70 GPa.

Roots of the transcendental equation
The first five positive root of the transcendental equation $J_1(\beta_m a)=0$ as defined in [16] are $\beta_1=3.8317$, $\beta_2=7.0156$, $\beta_3=10.1735$, $\beta_4=13.3237$, $\beta_5=16.470$.

Case 1:
$F(r,\varphi,z)=(r^2-a^2)^2(\varphi^2-\varphi_0^2)^2(z^2-h^2)^2$
i.e. the disk is initially at arbitrary temperature $F(r,\varphi,z)$.
Consider an instantaneous point heat source located at the position (r_1,φ_1,z_1) and releasing its entire energy spontaneously at instant $t\to\tau=5$ s, such a point source is related to the volumetric heat source $g(r,\varphi,z,t)$ that has the dimension W.m^{-3} by

$$g(r,\varphi,z,t)=g_p^i\,\frac{1}{r}\,\delta(r-r_1)\delta(\varphi-\varphi_1)\delta(z-z_1)\delta(t-\tau)$$

where δ is the Dirac-delta function and the point source $g_p^i=50$ J. m^{-1} represents the total quantity of energy released by the point source.
The term $\frac{1}{r}$ appearing in above equation is due to the scale factor associated with the transformation of the reciprocal of the volume element $\frac{1}{dV}$ from the cartesian to a curvilinear coordinate system, which in the case of the cylindrical coordinate system gives $\frac{1}{r}$.
Case 2:
$F(r,\varphi,z)=0$ i.e. the disk is initially at zero temperature.
Consider an instantaneous cylindrical surface heat source g_s^i located at the position (r',φ',z') and releasing it's entire energy spontaneously at the instant $t=\tau$.
Such a source is related to the volumetric heat source $g(r,\varphi,z,t)$ that has the dimension W.m^{-3} by

$$g(r,\varphi,z,t)=\frac{g_s^i}{2\pi r}\,\delta(r'-r_1)\delta(\varphi'-\varphi_1)\delta(z'-z_1)\delta(t'-\tau)$$

An instantaneous cylindrical surface heat source g_s^i has the dimensions $(Ws)/m$ or J/m, hence energy per unit length. In equation (8-61), the additional term appearing in the denominator is associated with the scale factor of the transformation. That is, g_s^i represents the strength of the cylindrical surface source per unit length, and the quantity $\frac{g_s^i}{2\pi r}$ represents the source strength per unit area.
substituting these values into the solution eq. (34), we obtain

$$\begin{aligned}
T(r,\varphi,z,t)=&\frac{g_i^s}{2\pi r}\sum_{m=1}^{\infty}\sum_{\nu}\sum_{p=1}^{\infty}K_1(\beta_m,r')\,K_0(\nu,\varphi')\,K(\eta_p,z')\,e^{-\alpha(\beta_m^2+\frac{\nu^2}{r^2}+\eta_p^2)t}\\
&\left\{\int_{t'=0}^{t}e^{\alpha(\beta_m^2+\frac{\nu^2}{r^2}+\eta_p^2)t'}\delta(t'-\tau)dt'\right.\\
&\left[\frac{\alpha}{k}\int_{r'=0}^{a}\int_{\varphi'=0}^{\varphi_0}\int_{z'=0}^{h}r'K_1(\beta_m,r')K_0(\nu,\varphi')K(\eta_p,z')\delta(r'-r_1)\delta(\varphi'-\varphi_1)\delta(z'-z_1)dr'd\varphi'dz'\right.\\
&+\frac{\alpha}{k}\,a\,K_1(\beta_m,a)\int_{\varphi'=0}^{\varphi_0}\int_{z'=0}^{h}K_0(\nu,\varphi')K(\eta_p,z')f_1(\varphi',z',t)d\varphi'dz'\\
&+\alpha\,\nu\sqrt{\frac{2}{\varphi_0}}\int_{r'=0}^{a}\int_{z'=0}^{h}r'K_1(\beta_m,r')K(\eta_p,z')f_2(r',z',t')dr'dz'\\
&-\alpha\,\nu\sqrt{\frac{2}{\varphi_0}}\cos(\nu\varphi_0)\int_{r'=0}^{a}\int_{z'=0}^{h}r'K_1(\beta_m,r')K(\eta_p,z')f_3(r',z',t')dr'dz'\\
&+\sqrt{\frac{2}{\pi}}\,\alpha\,\eta_p\int_{r'=0}^{a}\int_{\varphi'=0}^{\varphi_0}r'K_1(\beta_m,r')K_0(\nu,\varphi')f_4(r',\varphi',t')dr'd\varphi'\\
&\left.\left.+\sqrt{\frac{2}{\pi}}\,\alpha\,\eta_p\,\cos(\eta_p h)\int_{r'=0}^{a}\int_{\varphi'=0}^{\varphi_0}r'K_1(\beta_m,r')K_0(\nu,\varphi')f_5(r',\varphi',t')dr'd\varphi'\right]\right\}
\end{aligned}\tag{39}$$

The instantaneous cylindrical surface heat source is related to the volume heat source by means of Dirac-delta func-

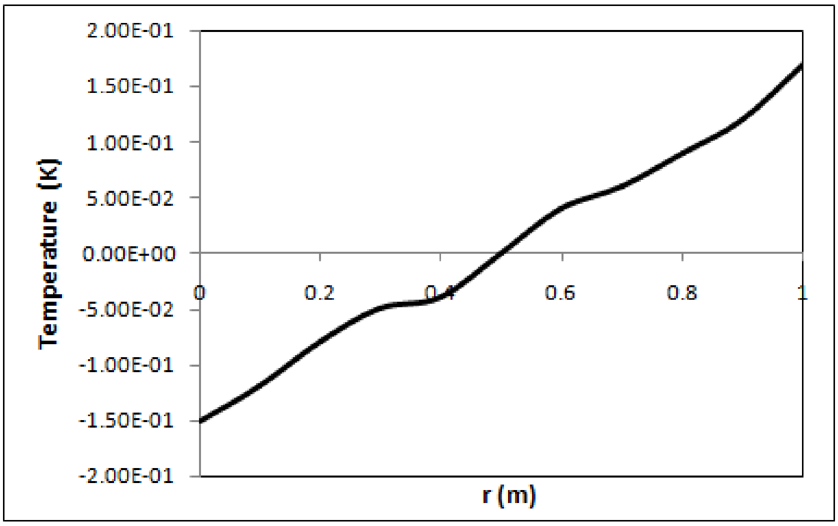

Fig. 2. The temperature changes T in the radial direction.

tion. Integration involving delta functions are immediately performed and Eq. (39) becomes

$$\begin{aligned}T(r,\varphi,z,t) = {} & \frac{g_i^s}{2\pi r}\sum_{m=1}^{\infty}\sum_{\nu}\sum_{p=1}^{\infty} K_1(\beta_m,r)\,K_0(\nu,\varphi)\,K(\eta_p,z)\,e^{-\alpha(\beta_m^2+\frac{\nu^2}{r^2}+\eta_p^2)(t-\tau)} \\ & \Big\{\frac{\alpha}{k} r_1 K_1(\beta_m,r_1)K_0(\nu,\varphi_1)K(\eta_p,z_1) \\ & +\frac{\alpha}{k}\,a\,K_1(\beta_m,a)\int_{\varphi'=0}^{\varphi_0}\int_{z'=0}^{h} K_0(\nu,\varphi')K(\eta_p,z')f_1(\varphi',z',t)d\varphi' dz' \\ & +\alpha\,\nu\sqrt{\frac{2}{\varphi_0}}\int_{r'=0}^{a}\int_{z'=0}^{h} r' K_1(\beta_m,r')K(\eta_p,z')f_2(r',z',t')dr'dz' \\ & -\alpha\,\nu\sqrt{\frac{2}{\varphi_0}}\cos(\nu\varphi_0)\int_{r'=0}^{a}\int_{z'=0}^{h} r' K_1(\beta_m,r')K(\eta_p,z')f_3(r',z',t')dr'dz' \\ & +\sqrt{\frac{2}{\pi}}\,\alpha\,\eta_p\int_{r'=0}^{a}\int_{\varphi'=0}^{\varphi_0} r' K_1(\beta_m,r')K_0(\nu,\varphi')f_4(r',\varphi',t')dr'd\varphi' \\ & +\sqrt{\frac{2}{\pi}}\,\alpha\,\eta_p\cos(\eta_p h)\int_{r'=0}^{a}\int_{\varphi'=0}^{\varphi_0} r' K_1(\beta_m,r')K_0(\nu,\varphi')f_5(r',\varphi',t')dr'd\varphi'\Big\}\end{aligned} \tag{40}$$

6. Discussion of the results

In this paper a circular sector disk is considered and determined the expressions of temperature, displacement and thermal stresses due to internal heat generation within it. As an illustration, we carried out numerical calculations for a circular sector disk made up of aluminum(pure) and examined the thermoelastic behavior in the state for the temperature, displacement and thermal stresses in the radial direction. The numerical calculation has been carried out with help of computational mathematical software Mathcad-2007, and the graphs are plotted with the help of Excel (MS Office-2007).
We examined two special case of our solution equation eq. (34).
(a): $F(r,\varphi,z) = (r^2-a^2)^2(\varphi^2-\varphi_0^2)^2(z^2-h^2)^2$
$g(r,\varphi,z,t) = g_p^i\,\delta(r-r_1)\delta(\varphi-\varphi_1)\delta(z-z_1)\delta(t-\tau)$
In this case, initially disk at arbitrary temperature with internal heat generation $g(r,\varphi,z,t)$ (W.m^{-3}) and the time dependent heat flux $f_1(\varphi,z,t)$ is applied on the fixed circular edge ($r=a$), while boundary surfaces at ($\varphi=0$), ($\varphi=\varphi_0$), ($z=0$) and ($z=h$) are kept temperatures $f_2(r,z,t)$, $f_3(r,z,t)$, $f_4(r,\varphi,t)$ and $f_5(r,\varphi,t)$ respectively. The heat source $g(r,\varphi,z,t)$ (W.m^{-3}) an instantaneous point heat source located at the position (r_1,φ_1,z_1) and releasing its entire energy spontaneously at instant $t\to\tau$, such a point source is related to the volumetric heat source by means of Dirac-delta function. The temperature distribution, displacement, thermal stresses are obtained in eqs. (34), (36)–(38).

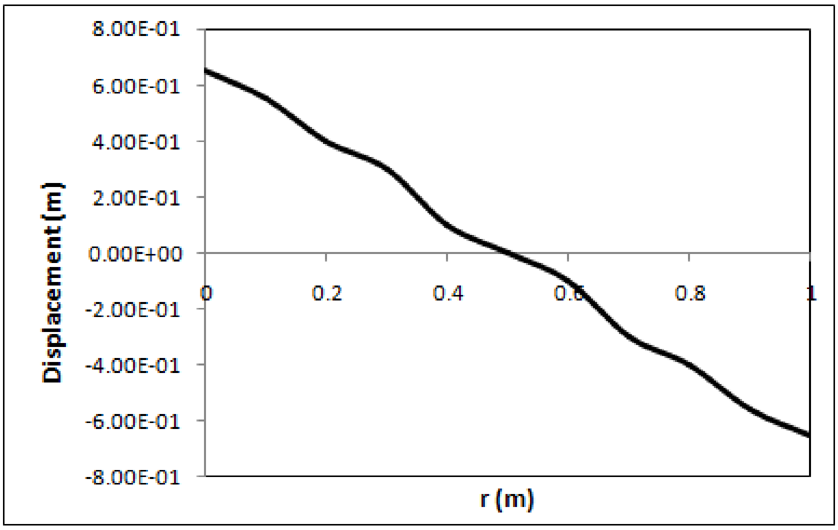

Fig. 3. The displacement function ψ in the radial direction.

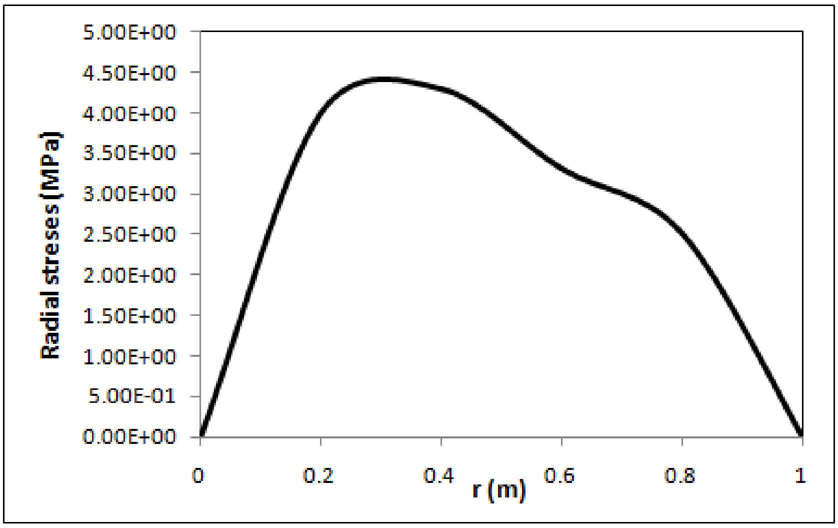

Fig. 4. The radial stress function σ_{rr} in the radial direction.

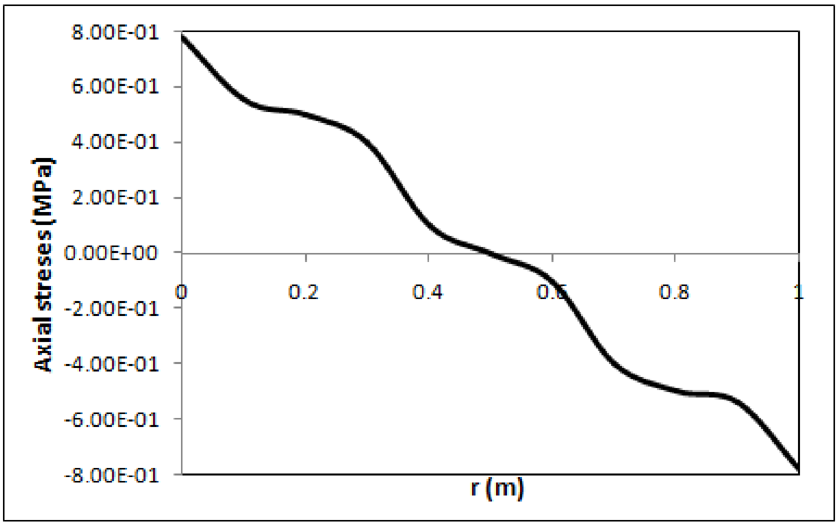

Fig. 5. The angular stress function $\sigma_{\theta\theta}$ in the radial direction.

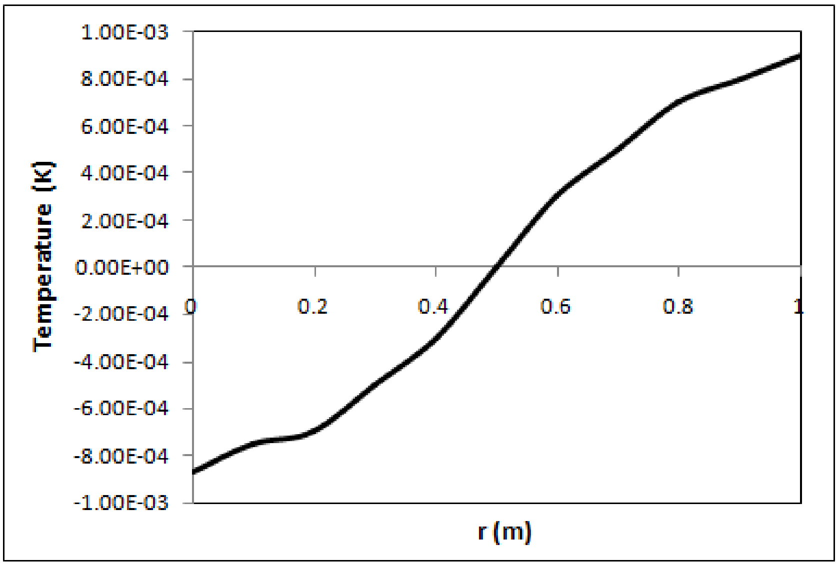

Fig. 6. The temperature changes T in the radial direction.

From Fig. 2, it is observed that due to the internal heat generation, the temperature function T increases non-uniformly from center $(r = 0)$ of a circular disk to outer circular edge $(r = 1)$. It becomes zero at $r = 0.5$.
From Fig. 3, it is clear that, the displacement function psi from the center of circular disk to outer circular edge and it becomes zero at $r = 0.5$.
From Fig. 4, it is observed that, due to the internal heat generation, the radial stress develops the tensile stress and becomes zero at the center $(r = 0)$ and outer circular edge $(r = 1)$.
From Fig. 5, it is clear that, due to the internal heat generation, the axial stress decreases from center $(r = 0)$ of a circular disk to outer circular edge $(r = 1)$. It becomes zero at $r = 0.5$.
(b): $F(r,\varphi,z) = 0$, $g(r,\varphi,z,t) = g_s^i\,\delta(r'-r_1)\delta(\varphi'-\varphi_1)\delta(z'-z_1)\delta(t'-\tau)$
In this case, zero initial temperature with internal heat generation $g(r,\varphi,z,t)$ (W.m^{-3}) and the time dependent heat flux $f_1(\varphi,z,t)$ is applied on the fixed circular edge $(r = a)$, while boundary surfaces at $(\varphi = 0)$, $(\varphi = \varphi_0)$, $(z = 0)$ and $(z = h)$ are kept temperatures $f_2(r,z,t)$, $f_3(r,z,t)$, $f_4(r,\varphi,t)$ and $f_5(r,\varphi,t)$ respectively. An instantaneous cylindrical surface heat source g_s^i located at the position (r',φ',z') and releasing it's entire energy spontaneously at the instant $t = \tau$, such a point source is related to the volumetric heat source by means of Dirac-delta function. The temperature distribution is obtained in eq. (40).
From Fig. 6, it observed that due to the internal heat generation, the temperature function T increases non-uniformly from center $(r = 0)$ of a circular disk to outer circular edge $(r = 1)$. It becomes zero at $r = 0.5$.

7. Concluding remarks

In the present article, we analyzed the quasi-static thermal stresses in a circular sector disk due to internal heat generation within it. The present method is based on the direct method, using the finite Hankel and the generalized finite Fourier transform and using their inversions. As an illustration, we carried out numerical calculations for a aluminum (pure) plate, with the material properties specified as above and examined the two special cases. In first case, initially disk at arbitrary temperature and the heat source $g(r,\varphi,z,t)$ (W.m^{-3}) an instantaneous point heat source located at the position (r_1,φ_1,z_1) and releasing its entire energy spontaneously at instant $t \to \tau$, such a point source is related to the volumetric heat source by means of Dirac-delta function. The temperature distribution, displacement, thermal stresses are obtained in eqs. (34), (36)–(38). In second case, initially the disk is at zero temperature and an instantaneous cylindrical surface heat source g_s^i located at the position (r',φ',z') and releasing it's entire energy spontaneously at the instant $t = \tau$, such a point source is related to the volumetric heat source by means of Dirac-delta function. The temperature distribution is obtained in eq. (40). We conclude that, the initial temperature changes only, the reflection of the temperature wave at the center may be neglected and the temperature may be obtained as if the disk were solid.
The obtained solution can be used in the numerical analysis of the field temperature of the disk as well as for an investigation of the thermally induced vibration of this disk. Also any particular case of special interest can be derived by assigning suitable values to the parameters and functions in the expressions (34)–(38).

References

[1] J.L. Nowinski, Theory of Thermoelasticity with Application, Sijthof Noordhoff, Alphen Aan Den Rijn, The Netherlands, (1978) 407.
[2] W. Nowacki, The State of Stresses in a Thick Circular Plate due to Temperature Field, Bull Acad Polon Sci, Ser Scl Tech, 5 (1957) 227.
[3] S.K. Roy Choudhury, A Note on the Quasi-Static Thermal Deflection of a Thin Clamped Circular Plate due to Ramp-Type of Heating of a Concentric Circular Region of the Upper Face, Journal of the Franklin Institute, 296 (1973) 213–219.
[4] P.C. Wankhede, On the Quasi-Static Thermal Stresses in a Circular Plate, Indian Journal of Pure and Applied Mathematics, 13 (1982) 1273–1277.
[5] M. Ishihara, Y. Tanigawa, R. Kawamura, N. Noda, Theoretical Analysis of Thermoelastoplastic Deformation of a Circular Plate due to a Partially Distributed Heat Supply, Journal of Thermal Stresses, 20 (1997) 203–225.
[6] N.L. Khobragade, K. C. Deshmukh, An Inverse Quasi-Static Thermal Deflection Problem for a Thin Clamped Circular Plate, Journal of Thermal Stresses, 28 (2005) 353–361.
[7] Y. Ootao, Y.Tanigawa, Transient Thermoelastic Analysis for a Functionally Graded Hollow Cylinder, Journal of Thermal Stresses, 29 (2006) 1031–1046.
[8] K C. Deshmukh, S. D. Warbhe, V. S. Kulkarni, Quasi-Static Thermal Deflection of a Thin Clamped Circular Plate due to Heat Generation, Journal of Thermal Stresses 32 (2009) 877–886.
[9] K.R. Gaikwad and K.P. Ghadle, Quasi-Static Thermoelastic Problem of an Infinitely Long Circular Cylinder, Journal of Korean Society for Industrial and Applied Mathematics, 14(3) (2010) 141-?149.
[10] K.S. Parihar, S.S. Patil, Transient Heat Conduction and Analysis of Thermal Stresses in Thin Circular Plate, Journal of Thermal Stresses, 34(4) (2011) 335-?351.
[11] K.R. Gaikwad, K.P. Ghadle, Nonhomogeneous Heat Conduction Problem and its Thermal Deflection due to Internal Heat Generation in a Thin Hollow Circular Disk, Journal of Thermal Stresses, 35(6) (2012) 485–498.
[12] K.R. Gaikwad, Analysis of Thermoelastic Deformation of a Thin Hollow Circular Disk Due to Partially Distributed Heat Supply, Journal of Thermal Stresses, 36(3) (2013) 207–224.
[13] R.M. Darji and M.G. Timol, Deductive group symmetry analysis for a free convective boundary-layer flow of electrically conducting non-Newtonian fluids over a vertical porous-elastic surface, Int. J. Adv. Appl. Math. and Mech. 1(1) (2013) 1–16.
[14] M. Gnaneswara Reddy, Heat and mass transfer effects on unsteady MHD flow of a chemically reacting fluid past an impulsively started vertical plate with radiation , Int. J. Adv. Appl. Math. and Mech. 1(2) (2013) 1–15.
[15] M.F. El-sayed, N.T.M. Eldabe, M.H. Haroun, D. M.Mostafa, Nonlinear stability of viscoelastic fluids streaming through porous medium under the influence of vertical electric fields producing surface charges, Int. J. Adv. Appl. Math. and Mech. 2(2) (2014) 110–125.
[16] M.N. Ozisik, Boundary Value Problem Of Heat Conduction, International Textbook Company, Scranton, Pennsylvania, 1968, 481–492.